Exploring the Structural Dynamics of Thin Films using X-ray Diffraction

Kendall Vanderhoof '20, and Frank Peiris, Ph.D.
Kenyon College Summer Science 2017

Abstract

Multiple thin films were scanned with an x-ray diffractometer and their diffraction peaks were analyzed to study their crystal phases and to use those crystal phases to discover more information about the zirconia (ZrO_2) and HgCdSe samples. The ZrO_2 samples were spin coated on silicon substrates and treated with oleic acid (OA) or trioctylphosphine oxide (TOPO) and annealed at various temperatures to influence their crystal phases. The TOPO samples were amorphous for longer, but transitioned from tetragonal to monoclinic before the OA samples. The second set of samples had different alloy concentrations of HgSe and CdSe, and were grown by molecular beam epitaxy (MBE) on GaSb and ZnTe/Si substrates. The diffraction peaks of HgCdSe were used to verify the alloy concentrations predicted by the MBE growth technique. In addition, these studies confirm that the samples are of high quality, deduced from the widths of the diffraction peaks in the x-ray spectra.

Background

ZrO_2

- ZrO_2 is spin coated on a silicon substrate

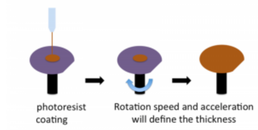

Figure 1. Schematic of spin coating [1]

- Samples are treated with trioctylphosphine oxide (TOPO) or oleic acid (OA), chemicals that bind the zirconia nanoparticles
- They are then annealed for 168 hours at various temperatures
- The annealing procedure and chemicals influence the crystal phases of the film
- Through X-ray Diffraction, we can determine the crystal-phase of the sample

HgCdSe

- HgCdSe is grown via molecular beam epitaxy (MBE) which produces more even samples than spin coating

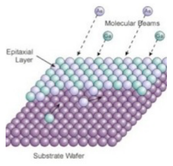

Figure 2. Schematic of MBE [2]

- Each sample has a goal percentage of HgSe and CdSe. Through calibrations, MBE determines the alloy concentrations; however, after samples are grown, the exact percentage needs to be calculated
- This can be done by using Vegard's Law; exploiting the linear dependence between the two lattice parameters of the compounds (see Fig. 3 & 4)

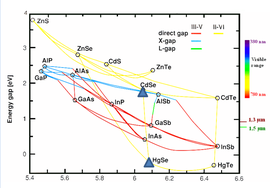

Figure 3. Energy gap vs. lattice parameter of several semiconductors [3]

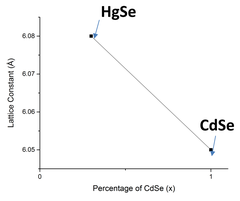

Figure 4. Vegard's Law shows the linear dependence of the lattice parameters

Approach

X-Ray Diffraction

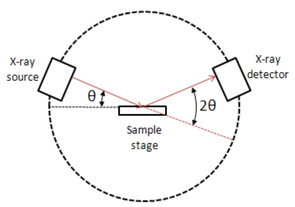

Figure 5. X-Ray Diffractometer stage [4]

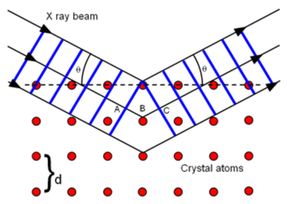

Figure 6. X-Ray Diffraction with crystal atoms [5]

Bragg's Law: $n\lambda = 2d \sin\theta$

- X-ray diffraction can find:
  - The lattice parameter (related to the distance between atoms)
  - The quality of the crystal
  - The crystal phase
  - The crystal structure

X-Ray Spectra of ZrO_2

TOPO

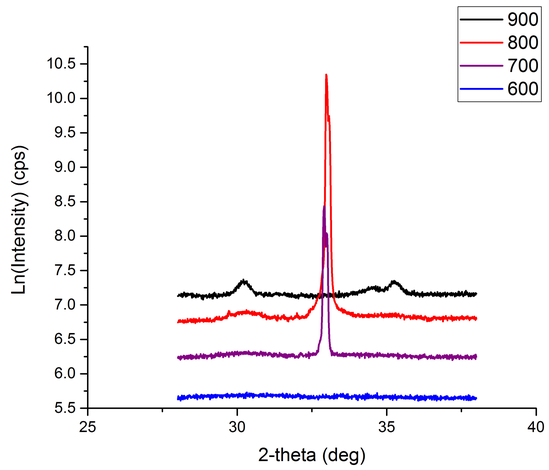

Figure 7. The TOPO samples are stacked from highest annealing temperature to lowest annealing temperature from top to bottom. Below 600 degrees, the absence of diffraction peaks indicate the samples are amorphous. The high intensity peak at 33 degrees is the substrate.

Oleic Acid

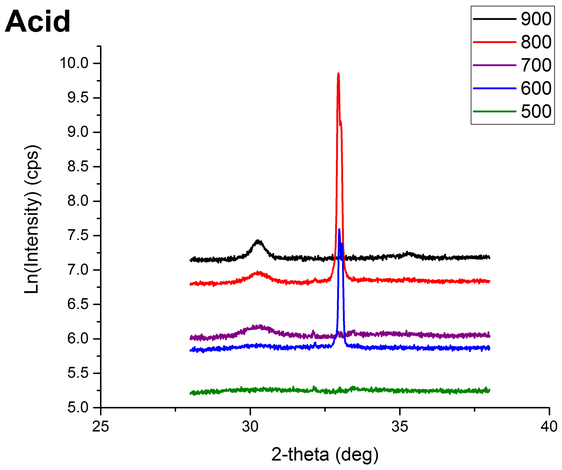

Figure 8. The OA samples are stacked from highest annealing temperature to lowest annealing temperature from top to bottom. Below 500 degrees, the absence of diffraction peaks indicates that the samples are amorphous. The high intensity peak at 33 degrees is the substrate.

- As shown in figures 7 & 8, samples below 700 degrees treated with TOPO, and below 600 degrees treated with oleic acid are observed to be amorphous.
- The tetragonal peaks appear around 30 degrees for all other samples.
- The monoclinic peaks are observed around 35 degrees, and can be seen in the 900 degree TOPO sample, and begin appearing in the 900 degree oleic acid sample.
- The width and height of the tetragonal peaks are shown in figures 10 & 11, which show the peaks gaining intensity as their annealing temperature increases.

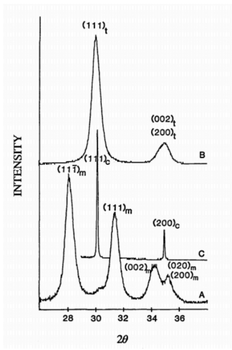

Figure 9. The graph shows the tetragonal, cubic and monoclinic peaks of zirconia. [6]

Phase Transformations of ZrO_2

- TOPO

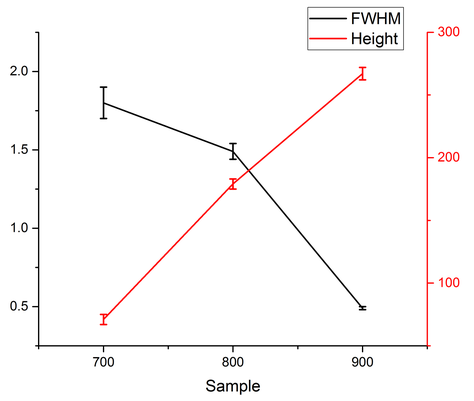

Figure 10. The tetragonal peaks of the TOPO samples were graphed, and their full widths at half minimum (FWHM) and peak heights (in red) were graphed above. The decrease in peak width and increase in peak height prove that the 900 peak is most tetragonal. Below 700, the samples were amorphous and are not included.

- Oleic Acid

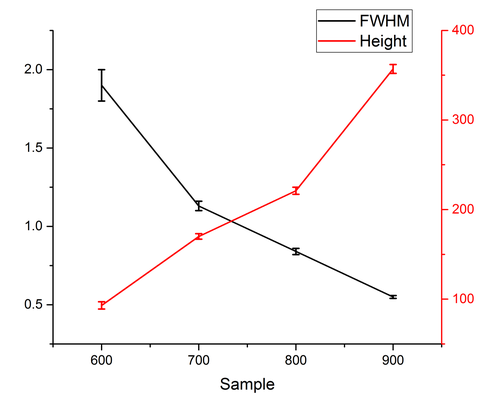

Figure 11. The tetragonal peaks of the OA samples were graphed, in the same way as the above TOPO samples, but the OA samples transitioned from amorphous to tetragonal before the TOPO samples did, so the 600 degree sample is included.

- The full width at half minimum of the intensity peaks is inversely related to the height of the intensity peaks; the peaks are becoming more defined as the annealing temperature increases, indicating that the zirconia is transforming its crystal phases inside the film.

HgCdSe Thin Films

Sample	X	a(nm)	%Δa
SZ0037	0.194	0.607418	0.423
SZ0074	0.306	0.607082	0.478
SZ0104	0.263	0.607211	0.457
SZ0109	0.245	0.607265	0.448
SZ0111	0.208	0.607376	0.430
SG0022	0.209	0.607373	0.364
SG0025	0.179	0.607463	0.349
SG0027	0.249	0.607253	0.384

Figure 12. The given x-values for each sample is the percentage of CdSe in each sample. Using the lattice constants of each sample's substrate, the percent difference in the lattice parameter of each sample is calculated.

- Finding the percentage a sample is different to it's substrate is important, because when their lattice constants are similar, their diffraction peaks show up on top of each other, making the sample hard to analyze.

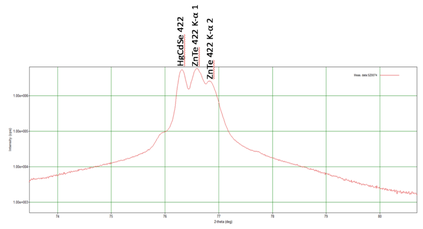

Figure 13. Sample SZ0074 was found to be the most different to its substrate, but its peaks are still on top of its substrate peaks.

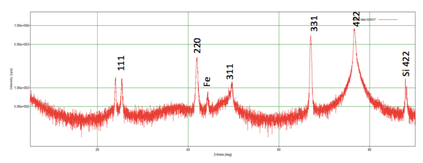

Figure 14. The entire spectra of sample SZ0037, which shows the iron plate peak, and the substrate peak on top of the 422 HgCdSe peak.

- The HgCdSe peaks were found to be on top of the substrate peaks, which doesn't allow one to calculate the actual percentages of HgSe and CdSe
- The goal of MBE is to grow samples on substrates that have lattice constants similar to them, to aid in growth.

References

1. Casquillas, Guilhem Velve, et al. "PDMS Membrane: Thickness of a Spin Coated PDMS Layer." *Elveflow*, www.elveflow.com/microfluidic-tutorials/soft-lithography-reviews-and-tutorials/introduction-in-soft-lithography/pdms-membrane-thickness-of-a-spin-coated-pdms-layer/.
2. Liu, Huiyun. "Molecular Beam Epitaxy." *London Centre for Nanotechnology*, www.london-nano.com/research-and-facilities/themes/techniques/molecular-beam-epitaxy.
3. Föll, H. "Ternary and Quarternary III-V's." *Semiconductor Technology*, www.tf.uni-kiel.de/matwis/amat/semitech_en/kap_2/backbone/r2_3_1.html.
4. Grebenkemper, Jason. "Powder X-Ray Diffraction." *Chemistry LibreTexts*, Libretexts, 16 Feb. 2017, chem.libretexts.org/Core/Analytical_Chemistry/Instrumental_Analysis/Diffraction_Scattering_Techniques/Powder_X-ray_Diffraction.
5. "X-Ray Diffraction." *Teaching Advanced Physics*, Institute of Physics, tap.iop.org/atoms/xray/530/page_47297.html.
6. Srinvasan, R., et al. "Identification of Tetragonal and Cubic Structures of Zirconia Using Synchronton x-Radiation Source." *University of Nebraska Lincoln*, 1991.

Acknowledgments

This work was funded by the Kenyon College Summer Science Scholars program. I would also like to thank Professor Frank Peiris for his assistance throughout the project.